Title: Cognitive Deficits and Altered Functional Brain Network Organization in Pediatric Brain Tumor Patients

Authors: Hari Anandarajah[1*], Benjamin A. Seitzman[2*], Alana McMichael[2], Ally Dworetsky[3], Rebecca S. Coalson[2,3], Catherine Jiang[4], Hongjie Gu[5], Dennis L. Barbour[4,6], Bradley L. Schlaggar[2,7,8,9], David D. Limbrick[10], Joshua B. Rubin[1,6], Joshua S. Shimony[3], Stephanie M. Perkins[11]
[*]These authors contributed equally to this work

Affiliations:
1. Department of Pediatrics, St. Louis Children's Hospital, Washington University School of Medicine, St. Louis, Missouri
2. Department of Neurology, Washington University School of Medicine, St. Louis, Missouri
3. Mallinckrodt Institute of Radiology, Washington University School of Medicine, St. Louis, Missouri
4. Department of Biomedical Engineering, Washington University in St. Louis, St. Louis, Missouri
5. Department of Biostatistics, Washington University School of Medicine, St. Louis, Missouri
6. Department of Neuroscience, Washington University School of Medicine, St. Louis, Missouri
7. Kennedy Krieger Institute, Baltimore, Maryland
8. Department of Neurology, Johns Hopkins University School of Medicine, Baltimore, Maryland
9. Department of Pediatrics, Johns Hopkins University School of Medicine, Baltimore, Maryland
10. Department of Neurological Surgery, Washington University School of Medicine, St. Louis, Missouri
11. Department of Radiation Oncology, Washington University School of Medicine, St. Louis, Missouri

Corresponding Author: Stephanie M. Perkins, sperkins@wustl.edu, 314-273-2931 (phone), 314-454-5628 (fax), 660 S. Euclid Ave, Campus Box 8224, St. Louis, Missouri, USA, 63110

Author Contributions:
Experimental Design: D.L.B., B.L.S., D.D.L., J.B.R., S.M.P.
Implementation: H.A., A.M., A.D., R.C., B.L.S., J.S.S., S.M.P.
Analysis: H.A, B.A.S., A.D., C.J., H.G., D.L.B., J.S.S.
Interpretation of Data: H.A., B.A.S., J.B.R., J.S.S., S.M.P.
Writing of Manuscript: All Authors

Abstract

Pediatric brain tumor survivors experience significant cognitive sequelae from their diagnosis and treatment. The exact mechanisms of these injuries are poorly understood, and validated predictors of cognitive outcome are lacking. The current study aims to determine if there are abnormalities in functional brain network organization and cognitive performance in pediatric brain tumor patients, measured via resting state functional magnetic resonance imaging (rsfMRI) and the NIH Toolbox Cognition Battery, respectively. Further, we assess potential relationships between changes in brain network architecture and behavior in the patients.

Patients ages 4-18 years old with diagnosis of a brain tumor underwent awake rsfMRI during regularly scheduled clinical imaging and were tested with the NIH Toolbox Cognition Battery. Overall, functional brain network organization was significantly different in patients compared to age- and sex-matched healthy controls ($p < 0.001$). Network integrity within the dorsal attention network was particularly affected, with 86% of patients having connectivity strength 2+ SD below the mean of controls ($p < 0.0001$). Moreover, cognitive testing of patients demonstrated significant impairments in multiple domains, including attention ($p < 0.05$, FDR corrected). Finally, a significant amount of variance of age-adjusted total composite scores from the Toolbox was explained by changes in segregation between the dorsal attention and default mode networks as well as sex ($R^2 = 0.52$, $p < 0.05$).

Pediatric brain tumor patients demonstrated statistically significant deficits in multiple cognitive domains and multiple abnormalities in brain network architecture. Thus, rsfMRI may provide insight into neural systems that underlie these changes in

cognitive function, suggesting that these metrics may serve as a biomarker for cognitive performance.

Keywords: pediatric brain tumor, brain networks, attention, cognition, brain-behavior

1. Introduction

Primary brain tumors are the most common solid tumors in childhood. With advances in treatment options, overall survival for pediatric brain tumors has significantly improved and the majority of patients become long-term survivors (Gajjar et al., 1997; Merchant et al., 2009; Packer et al., 2006). The presence of a Central Nervous System tumor increases the risk of cognitive impairment, with 20-50% of patients exhibiting such impairment at the time of diagnosis (Krull et al., 2018). In addition to experiencing cognitive deficits from the presence of the tumor, survivors of childhood brain tumors can develop sequelae from their diagnosis and from tumor directed therapies, such as surgery, chemotherapy, and radiotherapy. The sequelae can include cognitive and behavioral performance deficits, compromised employability, and diminished quality of life (Gupta and Jalali, 2017; King et al., 2017; Krull et al., 2018; Ris et al., 2019; Zeltzer et al., 2009). Compared to their siblings, survivors of pediatric brain tumors have a 45 fold increased risk of hearing impairment, 8 fold increased risk of visual impairment, and an 11 fold increased risk of unemployment (Gupta and Jalali, 2017). Survivors are also less likely to complete secondary education, live independently, or be married (Schulte et al., 2019).

The causes of long-term sequelae in pediatric brain tumors are likely multifactorial, including the structural presence of a tumor during development, hydrocephalus, effects of surgical interventions (e.g., primary tumor resection and shunt placement), the effects of chemotherapy on the developing brain, and the well-documented effects of cranial radiotherapy in children (Hardy et al., 2018; Krull et al., 2018). Sex may also influence

long-term effects for survivors, as female pediatric brain tumor survivors generally demonstrate greater improvement post-treatment than males (Bledsoe et al., 2019). However, the precise mechanisms of these injuries are poorly understood, and validated predictors of cognitive outcomes are lacking.

Pediatric brain tumor patients undergo serial magnetic resonance imaging (MRI) during their course of treatment and follow-up. Resting state functional MRI (rsfMRI), which can be acquired during clinical imaging, may be a potential modality to assess changes in functional brain network organization that relate to cognitive performance in pediatric brain tumor patients (Matthews et al., 2006).

rsfMRI measures spontaneous changes in the blood-oxygen-level-dependent (BOLD) signal across the whole brain (Kazumata et al., 2017; Leuthardt et al., 2018; Power et al., 2011; Roland et al., 2017). rsfMRI studies in humans have identified anatomically separate, distributed regions of the brain that are functionally linked via strong correlations in these on-going BOLD signals (van den Heuvel and Hulshoff Pol, 2010). Such sets of regions form functional brain networks. There is convergent evidence from multiple human and animal studies for the following networks: somatomotor dorsal, somatomotor ventral, cingulo-opercular, auditory, default mode network, parietal memory, visual, frontoparietal, salience, ventral attention network, dorsal attention network (DAN), and reward (Seitzman et al., 2019).

A strength of rsfMRI is that spontaneous BOLD fluctuations can be acquired without requiring patients to perform a task. This freedom from task performance is

advantageous over task-based fMRI for testing in young children and patients with cognitive impairments, who may be unwilling or unable to perform adequately on tasks in the scanner. Importantly, rsfMRI, in tandem with network analytic tools, can be used to map the functional network architecture of the brain. Atypical network organization has consistently been identified in patients with brain disorders, including, but not limited to, Alzheimer Disease, Temporal Lobe Epilepsy, and Attention Deficit Hyperactivity Disorder (Fair et al., 2012; Hojjati et al., 2019; Shah et al., 2018).

Formal cognitive assessment by a neuropsychologist, while important for determining clinical care needs, is an expensive and time-consuming assessment for research studies. Utilization of a computer-based cognitive assessment is more feasible in the research setting. The NIH Toolbox Cognition Battery offers a good assessment of cognition that can easily be incorporated into a variety of clinical settings. The assessment is designed to measure executive function, attention, episodic memory, working memory, language, and processing speed for patients ages 3-85 years, and normative data is provided with adjustments for age, sex, race, and parental level of education (Akshoomoff et al., 2014). In this study, we prospectively obtained rsfMRI during routine clinical scanning and evaluated cognitive performance with the NIH Toolbox Cognition Battery in pediatric brain tumor patients.

2. Material and Methods

2.1. Participants

Study subjects included patients seeking care at St. Louis Children's Hospital who were enrolled after informed consent to prospectively undergo resting state functional MRI (rsfMRI) during regularly scheduled clinical imaging along with NIH Toolbox Cognition Battery testing. Eligibility for study entry was age 4-18 years old with diagnosis of any type of brain tumor. Subjects could be newly diagnosed, currently under treatment, or in the follow-up period after completion of treatment. Exclusion criteria were patients with a life expectancy less than one year or patients who were unable to complete cognitive testing due to non-cooperation or motor/visual deficits. The study was approved by the Washington University Institutional Review Board.

2.2. rsfMRI Acquisition

All subjects underwent awake, unsedated imaging as part of their routine clinical care. For the rsfMRI scans, subjects were instructed to lie still with eyes open during a period of rest. No auditory or visual stimuli were presented. Scans were obtained in a clinical setting to reduce the cost and time limitations found with obtaining separate research scans. Scans were acquired at various times, including pre-operatively (1), after surgery alone (1), and after surgery plus other treatment modalities, such as chemotherapy and/or radiotherapy (19).

T1-weighted, T2-weighted, and blood-oxygen level-dependent (BOLD) contrast sensitive images were obtained on a Siemens Trio 3T scanner. For the BOLD images,

gradient-echo echo-planar imaging with a repetition time (TR) of 2.07s, an echo time (TE) of 25ms, and a flip angle of 90° was used. Two 7-minute runs were acquired, covering the brain in 36 slices (4mm^3 isotropic voxels) (Fox et al., 2009; Pizoli et al., 2011).

An extant dataset of typically developing children were used to pair each study subject with an age- and sex-matched control. Control data were obtained on a separate Siemens Trio 3T Scanner with very similar acquisition parameters (TR = 2.5s, TE = 27ms, flip angle of 90°, 4mm^3 isotropic voxels) (Greene et al., 2014).

2.3. Preprocessing

To account for magnetization equilibrium and an auditory evoked response, the first 12 frames of each BOLD run were discarded (Laumann et al., 2015). Slice timing compensation was applied. Then, all BOLD images (for a single subject) were aligned to the first frame of the first run, 3D-cross realigned, and normalized (whole-brain mode of 1000). Then, all images resampled (3mm^3 voxels), registered to the high-resolution T1-weighted and T2-weighted anatomical images, and then to the Talairach atlas in a one-step operation (Buckner et al., 2004; Fonov et al., 2011; Smith et al., 2004).

Nuisance regression was carried out with regressors extracted from individually-defined ventricles, white matter, and the global mean signal, as well as the 6 parameters from

the motion correction step, all of which were submitted to Volterra expansion (Fox et al., 2009; Friston et al., 1996; Power et al., 2014).

To reduce the impact of motion artifacts, which is particularly important for measuring brain-behavior correlations, frame censoring was implemented. As previously described, all frames with framewise displacement exceeding 0.1mm after applying a low-pass filter on motion parameters were excluded (Fair et al., 2020; Siegel et al., 2017). Frame segments with fewer than 3 continuous frames were also censored. Each BOLD run was required to have a minimum of 30 low-motion frames, and participants with less than a total of 5 minutes of low-motion rsfMRI data were excluded from further analyses (Pizoli et al., 2011). The Washington University NeuroImaging Laboratory 4dfp Suite (https://4dfp.readthedocs.io/en/latest/) and MATLAB (R2015, Natick, MA) were used for all image processing.

A total of 21 study subjects and 21 age- and sex-matched healthy controls were considered for all further analyses.

2.4. Functional Brain Network Analysis

Conventional region of interest (ROI) seed-based functional connectivity analysis was performed on the preprocessed rsfMRI data. Functionally-defined ROIs representing “canonical” functional brain networks and regions of the basal ganglia, thalamus, cerebellum, amygdala, and hippocampus were used (Seitzman et al., 2020). Thus, for

each patient and control, a correlation matrix was generated. The matrix was sorted into functional networks (defined *a priori*). This matrix represents functional brain network organization for each subject. All ROIs overlapping with either the tumor or resection cavity were excluded from all analyses (replaced with the NaN operator in MATLAB). For some analyses, individual subject correlation matrices were Fisher-Z transformed and averaged together (study subjects and controls in separate groups).

2.5. NIH Toolbox Cognition Battery

All study subjects underwent neurocognitive testing via the NIH Toolbox Cognition Battery. Cognitive testing was performed within 6 months of the rsfMRI. Testing was performed in the hospital or clinic setting in a quiet and private environment. All testing was performed with an iPad as prescribed by the NIH Toolbox standard procedures. Test order was standardized by utilizing the same order of tests for all study subjects: Picture Vocabulary Test, Flanker Inhibitory Control and Attention Test, List Sorting Working Memory Test, Dimensional Change Card Sort Test (executive functioning), Pattern Comparison Test (processing speed), Picture Sequence Memory Test (episodic memory), and Oral Reading Recognition Test.

The age-adjusted scores for each measure were exported and analyzed. Additionally, a total of three composite scores were also analyzed. The Fluid Cognition Composite score includes the fluid ability measures (Flanker, Dimensional Change Card Sort (executive functioning)), Picture Sequence Memory (episodic memory), List Sorting Working Memory, and Pattern Comparison. This composite assesses fluid intelligence, which is thought to reflect the ability to learn new tasks or perform known tasks in new

situations. The NIH Toolbox Crystallized Composite score includes the Picture Vocabulary Test and the Oral Reading Recognition Tasks, which measure previously learned tasks. The total composite Score includes all of the administered tests.

2.6. Statistical Analyses

2.6.1. Brain Networks

For the rsfMRI data, a previously developed omnibus statistical test for functional networks (correlation matrices) was used (La Rosa et al., 2016). Briefly, the technique performs a non-parametric permutation test to determine whether the weighted correlation matrices are significantly different between groups (in this case, study subjects versus age- and sex-matched controls). Then, a post-hoc permutation test was implemented to determine the specific network blocks that were significantly different between groups (Gratton et al., 2019). For each test, 1000 bootstrapped samples were run, and False Discovery Rate (FDR) correction was applied to the post-hoc analysis.

Within-network connectivity, a measure of the internal correlation within a given network, was analyzed for the following networks : somatomotor dorsal, somatomotor ventral, cingulo-opercular, auditory, default mode network, parietal memory, visual, frontoparietal, salience, ventral attention network, DAN, and reward. Within-network connectivity was compared between study subjects and controls using a two-sample t-test. All correlations within a given network were Fisher-Z transformed and then averaged prior to the t-test. Study subjects with within-network connectivity 2 standard deviations below the mean of controls or more were considered abnormal.

2.6.2. Behavior and Brain-Behavior Relationships

The mean age-adjusted scores of the study subjects were compared to a normative sample via a one-sample t-test (significance level of 0.05 after FDR correction). All NIH Toolbox Cognition Battery scores, including the total composite, are normalized to have a mean of 100 with 1 SD at 15 (85/115) and 2 SD at 30 (70/130).

To explore the relationship between functional brain network organization and cognitive performance, multilinear regression was implemented in MATLAB. The total composite age-adjusted score for each study subject was selected as the dependent variable. The predictors matrix of independent variables included mean correlation values from network blocks that were found to be significantly different between groups. Since the DAN showed the largest change in study subjects (see Section 3.1.), only significant network blocks involving the DAN were considered in order to minimize multiple comparisons and to avoid a rank-deficient predictors matrix (due to the small number of subjects). Sex was added to the predictors matrix as a covariate.

3. Results

A total of 21 children with a primary brain tumor diagnosis and 21 age- and sex-matched controls were analyzed. All known subject demographics, including sex, age at time of scan, race, and ethnicity are presented in **Table 1**, as well as tumor diagnosis, tumor location, and treatment modalities for study subjects. The median time of rsfMRI acquisition was 20 months after diagnosis (range 0 months - 141 months), with only one acquisition occurring less than 7 months after diagnosis. The mean and median time

between acquisition of rsfMRI and the NIH Toolbox was 13 and 0 days, respectively, (range 0-178 days) and exceeded 8 days in only two study subjects.

Table 1: Subject Demographics

Control Subjects	**Female (N=5)**	**Male (N=16)**
Median age at time of scan (range)	10.6 (8.4-18.1)	12.6 (9.5-18.6)
Race		
- White	4	13
- Black/African American	0	1
- Unknown	1	2
Ethnicity		
- Non-Hispanic	4	16
- Hispanic	1	0
Study Subjects	**Female (N=5)**	**Male (N=16)**
Median age at time of scan (range)	10.7 (8.3-17.9)	12.6 (8.9-18.9)
Median tumor diagnosis age (range)	7.4 (5.0-13.7)	9.8 (1.6-17.9)
Race		
- White	4	12
- Black/African American	1	4

Ethnicity		
- Non-Hispanic	5	15
- Hispanic	0	1
Tumor Diagnosis		
- Astrocytoma of Cerebellum	0	1
- Craniopharyngioma	1	3
- Ependymoma	0	2
- Ganglioglioma	0	1
- Glioma	0	1
- Medulloblastoma	0	3
- Pilocytic Astrocytoma	3	2
- Pineal Mass	0	1
- Pineal Papillary	1	0
- Pineoblastoma	0	1
- Suprasellar/Third Ventral Mass	0	1
Tumor Location		
- Infratentorial	1	10
- Supratentorial	4	6
Specific Tumor Location		
- Brainstem	1	2
- Cerebellum	0	8
- Pineal	1	2
- Suprasellar	2	4
- Thalamus	1	0

Treatment		
- N/A (Pre-Operative)	0	1
- Surgery	0	1
- Surgery + Chemotherapy/Targeted Agent*	2	3
- Surgery + RT	3	8
- Trimodality	0	3

RT = Radiotherapy, Trimodality = Surgery + RT + Chemotherapy, *Vemurafenib

3.1. Functional brain network organization is significantly affected in pediatric brain tumor patients

There was a significant difference (t = 12.2, p = 4.2x10^{-38}) in the mean framewise displacement between the study (0.28 +/- 0.47mm) and control (0.20 +/- 0.34mm) subjects. However, after implementing a strict frame censoring threshold, there was no significant difference (t = 0.69, p = 0.49) in the number of frames retained between study (259 +/- 76) and control (240 +/- 100) subjects.

Within-network connectivity analysis of 12 cortical functional networks was performed. Compared to controls, study subjects demonstrated average within-network connectivity scores greater than 2 SD below the control subject mean in the cingulo-opercular, default mode, parietal memory, salience, and dorsal attention networks (**Fig 1**) at a significantly higher rate than expected (p < 0.0001). The dorsal attention network had the largest within-network connectivity deficit for study subjects compared to controls,

with 86% of study subjects having an absolute connectivity score greater than 2 SD below the mean of control subjects.

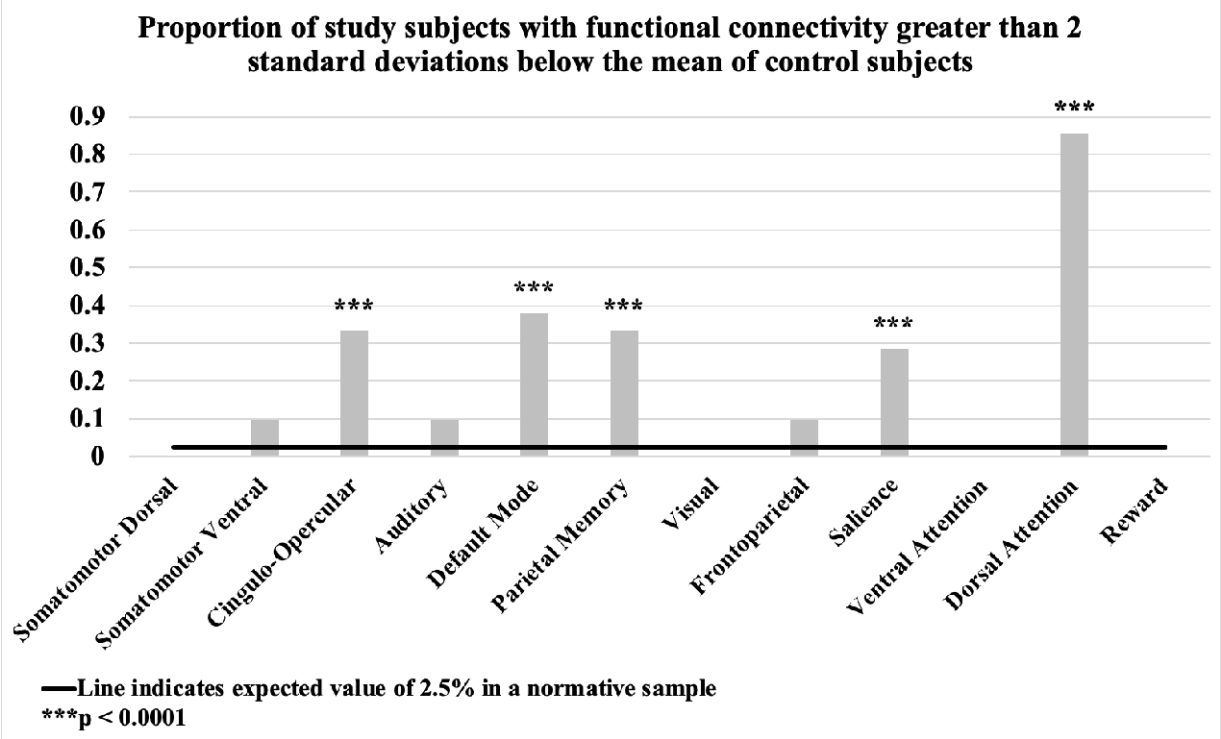

Fig 1: Within-network connectivity in pediatric brain tumor patients. The proportion of patients with functional connectivity greater than 2 SD below the mean of control subjects for 12 selected resting state networks (*** $p < 0.0001$).

There was a significant difference ($p < 0.001$) in overall functional brain network organization between the study and control subjects (**Fig 2A**). Post-hoc analysis revealed that the specific within- and between-network effects ($p < 0.05$, FDR corrected) were within the cingulo-opercular, default mode, parietal memory, salience, dorsal attention, and medial temporal lobe networks, and between the cingulo-opercular and default mode, cingulo-opercular and visual, cingulo-opercular and dorsal attention, cingulo-opercular and reward, auditory and default mode, auditory and visual, auditory and reward, default mode and parietal memory, default mode and visual, default mode and salience, default mode and ventral attention, default mode and dorsal attention,

parietal memory and dorsal attention, visual and salience, visual and ventral attention, salience and medial temporal lobe, salience and reward, and medial temporal lobe and reward networks. There were also significant differences within the thalamus, within the cerebellum, between the reward network and thalamus, and between the reward network and basal ganglia (**Fig 2B; Table 2**).

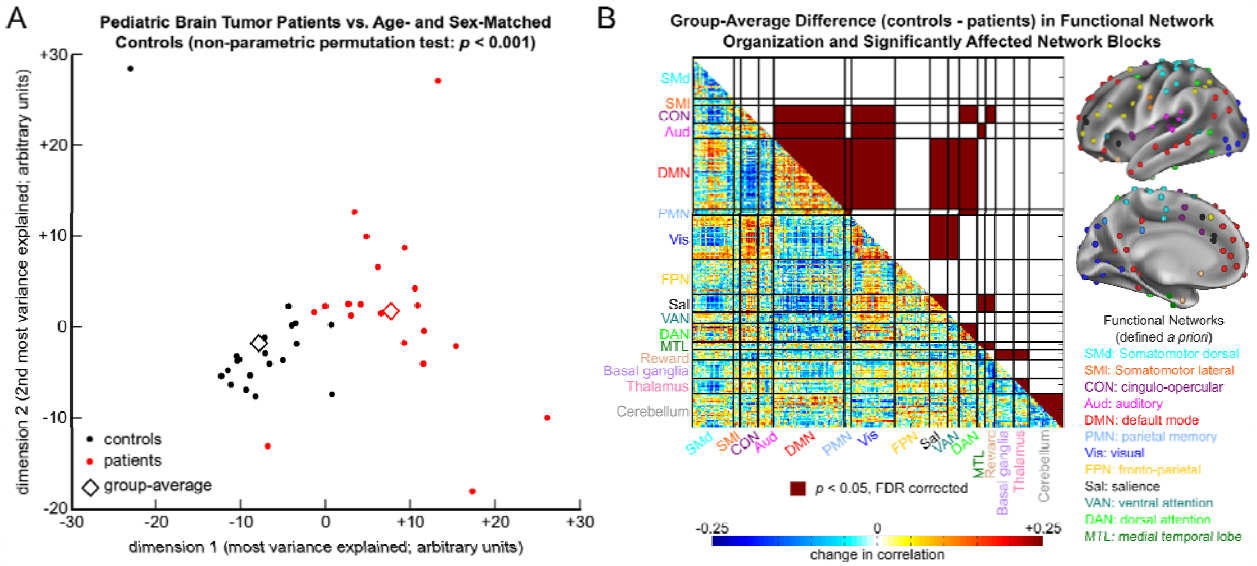

Fig 2: Functional brain network organization in pediatric brain tumor patients. (A) The difference between pediatric brain tumor patients (red) and age- and sex-matched controls (black) is displayed. Each filled dot represents the entire correlation matrix (functional network) of a single subject in a multidimensional space, with the group-average for patients and controls represented by diamonds. The two dimensions explaining the most variance in the full dataset are shown. The groups were significantly different ($p < 0.001$) per a non-parametric permutation test designed for correlation matrices. **(B)** The lower triangle of the matrix displays the group-average difference (controls minus patients) in rsfMRI at each region of interest (ROI). Filled blocks in the upper triangle of the matrix indicate significantly different network blocks between groups ($p < 0.05$, FDR corrected). Solid black lines delineate the functional networks (defined *a priori*) and non-cortical structures (the basal ganglia, thalamus, and cerebellum). Cortical ROIs included are displayed on the brain to the right and are color-coded according to their functional network membership.

Table 2: Significantly Affected Network Blocks

Network Block (stronger in controls)	P-Value †	Network Block (stronger in patients)	P-Value †
Between cingulo-opercular and visual	<0.001	Between cingulo-opercular and default mode	<0.001
Within default mode	<0.001	Between reward and basal ganglia	<0.001
Within parietal memory	<0.001	Between default mode and salience	<0.001
Within dorsal attention	<0.001	Between medial temporal lobe and reward	<0.001
Between visual and salience	<0.001	Between default mode and dorsal attention	<0.001
Within salience	<0.001	Between auditory and default mode	<0.001
Between visual and ventral attention	<0.001	Between parietal memory and dorsal attention	<0.001
Between default and parietal memory	0.009	Between default mode and ventral attention	<0.001

Between auditory and visual	0.022	Between default mode and visual	0.009
Between cingulo-opercular and dorsal attention	0.039	Between reward and thalamus	0.016
Within medial temporal lobe	0.028	Between cingulo-opercular and reward	0.022
		Within thalamus	0.022
		Within cerebellum	0.035
		Between salience and reward	0.035
		Between salience and medial temporal lobe	0.035
		Between auditory and reward	0.044

† (all values are FDR corrected)

3.2. Cognitive performance is significantly affected in pediatric brain tumor patients and related to brain network organization

Significant deficits ($p < 0.05$, FDR corrected) were found in the domains of attention/inhibition, cognitive flexibility, and episodic memory, as well as the fluid composite and total composite scores, when comparing study subjects to the normative mean (**Table 3**). A multilinear regression model explained a significant (F = 3.2, $p <$

0.05) amount of variance (R^2 = 0.52) of the age-adjusted total composite scores of the study subjects. The only significant predictors were average functional connectivity between the dorsal attention and default mode networks (□ = -219.7, 95% CI = [-414.1, -25.3]) and sex (female; □ = +17.7, 95% CI = [6.4, 29.0]). Thus, both stronger negative connectivity between the default mode and dorsal attention networks and female sex were associated with higher total composite scores from the NIH Toolbox Cognition Battery.

Table 3: NIH Toolbox Age-Adjusted Scores

Domain/Test	Mean ± STD	95% CL Mean	Range	P-Value †
Attention/Inhibition	85.67 ± 10.07	(81.08, 90.25)	[63-104]	**<0.0001**
Processing Speed	89.43 ± 26.05	(77.57, 101.3)	[54-146]	0.0777
Cognitive Flexibility	87.38 ± 13.63	(81.18, 93.58)	[60-113]	**0.0004**
Episodic Memory	92.24 ± 12.36	(86.61, 97.87)	[74-113]	**0.0093**
Oral Reading	94.71 ± 11.98	(89.26, 100.2)	[80-125]	0.0568
Working Memory	102.81 ± 13.95	(96.46, 109.2)	[75-144]	0.3671
Vocabulary	101.71 ± 13.05	(95.78, 107.7)	[77-131]	0.5538
Fluid Composite	86.05 ± 14.18	(79.59, 92.50)	[62-112]	**0.0002**
Crystalized Composite	97.90 ± 11.51	(92.67, 103.1)	[79-122]	0.0777
Total Composite	90.24 ± 12.55	(84.52, 95.95)	[71-115]	**0.0019**

† **Bold indicates significance (*p* < 0.05, FDR corrected)**

4. Discussion

The present study evaluated rsfMRI and computer-based neurocognitive assessment using the NIH Toolbox Cognition Battery for awake pediatric brain tumor patients. Prior research has revealed that pediatric brain tumor survivors face an increased risk for neurocognitive impairment both pre- and post-treatment (Hardy et al., 2018; Krull et al., 2018).

4.1. Brain network architecture and cognitive performance are disrupted in pediatric brain tumor patients

Overall, functional brain network organization was significantly different in study subjects compared to control subjects. Disruptions were observed within and between many networks, particularly within the dorsal attention network (DAN), in study subjects compared to age- and sex-matched controls. Specifically, the connectivity strength within the dorsal attention network (DAN) was greater than 2 SD below the mean of the control subjects for 86% of the study subjects. We found corroborating evidence of poorer cognitive performance in the domains of cognitive flexibility, episodic memory, and attention/inhibition in the study subjects. Furthermore, there was decreased segregation between the DAN and the default mode network in study subjects. This decrease in network segregation, in addition to sex, explained a significant amount of variance in cognitive performance.

4.2. The dorsal attention network is particularly affected

The findings of our study revealed significant deficits in the cognitive domain of attention, among others, in the study subjects. Likewise, patients' functional network architecture was disrupted, particularly in the DAN and its relationships with other networks. The DAN is the brain network responsible for top-down control of goal directed attention (Corbetta and Shulman, 2002; Fox et al., 2006; Posner and Petersen, 1990). Thus, it is reasonable to observe deficits in both attention-related behavior and attention network organization.

There was a significant decrease in the segregation between the DAN and the default mode network, the two most anticorrelated functional networks of the human brain (Fox et al., 2009). Intriguingly, the extent to which this specific network segregation was intact was significantly related to cognitive performance. This latter finding is concordant with previously published evidence from adult survivors of stroke, which revealed that longitudinal post-stroke recovery of cognitive functions correlates with the return of network segregation, and is also consistent with the importance of maintaining appropriate network segregation in healthy aging (Chan et al., 2018; Siegel et al., 2018). Here, patients with poor segregation between the DAN and default mode network showed worse cognitive decline. These results indicate that the integrity of functional network architecture in pediatric brain tumor patients may be behaviorally meaningful. However, the mechanisms of cognitive decline in these patients are likely multifactorial and require further investigation.

4.3. Future directions and limitations

The findings from this study are impactful and highlight the need for further study of rsfMRI in pediatric brain tumor patients. Survivors of childhood brain tumors experience significant neurologic sequelae from their diagnosis and treatment. rsfMRI is a non-invasive method of analyzing brain organization, capitalizing on synchronized neural activity that occurs between functionally related brain regions, in health and disease. The implications of the present data are that rsfMRI may provide valuable information regarding brain organization and its relationship with cognitive performance in pediatric brain tumor patients.

The strengths of this study include its prospective nature, the novel use of rsfMRI in pediatric brain tumor patients, and the temporally correlated assessment of cognition. The results also demonstrate the ability to obtain quality rsfMRI data in the clinical environment, which is of great significance for future use of this technology in pediatric brain tumor patients. Weaknesses of the study include the lack of longitudinal follow-up rsfMRI data and the small number of subjects. Additionally, there is significant heterogeneity in our study subjects with a wide variety of brain tumors, treatment modalities, and ages. Moreover, the data presented here are cross-sectional and, thus, it is difficult to appreciate fully the long-term relationship between functional brain network organization and cognitive performance. Furthermore, deeper assessment of attention in pediatric brain tumor patients (e.g., the Posner task), with the addition of pertinent clinical factors such as tumor type, size, location, and treatment, may be revealing. Lastly, rsfMRI and neurocognitive assessment occur at various times from

diagnosis to follow-up. Given the small study size, we were limited in our ability to evaluate known factors affecting cognition, such as hydrocephalus and treatment modalities (e.g., radiotherapy).

5. Conclusions

rsfMRI is a non-invasive tool that is able to measure the functional network architecture of the human brain. An important aspect of rsfMRI is that it can be successfully performed in pediatric brain tumor patients during routine clinical imaging. In the present work, patients' functional network organization was significantly different than controls, particularly in the dorsal attention network. Similarly, patients demonstrated poor performance on measures of goal-directed attention, among others. Finally, the integrity of functional network architecture was related to overall cognitive decline. Future work with a larger cohort of patients will allow for further study of rsfMRI as a potential tool for evaluation of changes to the brain of children with brain tumors and their long-term cognitive sequelae.

Acknowledgements

Research reported in this publication was supported by the Eunice Kennedy Shriver National Institute of Child Health & Human Development of the National Institutes of Health under Award Number U54 HD087011 to the Intellectual and Developmental Disabilities Research Center at Washington University and the Children's Discovery Institute.

Conflicts of Interest

D.L.B. has equity ownership in Bonauria, L.L.C. All other authors declare no competing interests.

References

Akshoomoff, N., Newman, E., Thompson, W.K., McCabe, C., Bloss, C.S., Chang, L., Amaral, D.G., Casey, B.J., Ernst, T.M., Frazier, J.A., Gruen, J.R., Kaufmann, W.E., Kenet, T., Kennedy, D.N., Libiger, O., Mostofsky, S., Murray, S.S., Sowell, E.R., Schork, N., Dale, A.M., Jernigan, T.L., 2014. The NIH Toolbox Cognition Battery: results from a large normative developmental sample (PING). Neuropsychology 28, 1–10. https://doi.org/10.1037/neu0000001

Bledsoe, J.C., Breiger, D., Breiger, M., Shonka, S., Ermoian, R.P., Ojemann, J.G., Werny, D.M., Leary, S.E.S., Geyer, J.R., 2019. Differential Trajectories of Neurocognitive Functioning in Females versus Males Following Treatment for Pediatric Brain Tumors. Neuro. Oncol. https://doi.org/10.1093/neuonc/noz092

Buckner, R.L., Head, D., Parker, J., Fotenos, A.F., Marcus, D., Morris, J.C., Snyder, A.Z., 2004. A unified approach for morphometric and functional data analysis in young, old, and demented adults using automated atlas-based head size normalization: reliability and validation against manual measurement of total intracranial volume. Neuroimage 23, 724–738. https://doi.org/10.1016/j.neuroimage.2004.06.018

Chan, M.Y., Na, J., Agres, P.F., Savalia, N.K., Park, D.C., Wig, G.S., 2018. Socioeconomic status moderates age-related differences in the brain's functional network organization and anatomy across the adult lifespan. Proc. Natl. Acad. Sci. U. S. A. 115, E5144–E5153. https://doi.org/10.1073/pnas.1714021115

Corbetta, M., Shulman, G.L., 2002. Control of goal-directed and stimulus-driven attention in the brain. Nat. Rev. Neurosci. 3, 201–215. https://doi.org/10.1038/nrn755

Fair, D.A., Miranda-Dominguez, O., Snyder, A.Z., Perrone, A., Earl, E.A., Van, A.N., Koller, J.M., Feczko, E., Tisdall, M.D., van der Kouwe, A., Klein, R.L., Mirro, A.E., Hampton, J.M., Adeyemo, B., Laumann, T.O., Gratton, C., Greene, D.J., Schlaggar, B.L., Hagler, D.J., Jr, Watts, R., Garavan, H., Barch, D.M., Nigg, J.T., Petersen, S.E., Dale, A.M., Feldstein-Ewing, S.W., Nagel, B.J., Dosenbach, N.U.F., 2020. Correction of respiratory artifacts in MRI head motion estimates. Neuroimage 208, 116400. https://doi.org/10.1016/j.neuroimage.2019.116400

Fair, D.A., Nigg, J.T., Iyer, S., Bathula, D., Mills, K.L., Dosenbach, N.U.F., Schlaggar, B.L., Mennes, M., Gutman, D., Bangaru, S., Buitelaar, J.K., Dickstein, D.P., Di Martino, A., Kennedy, D.N., Kelly, C., Luna, B., Schweitzer, J.B., Velanova, K., Wang, Y.-F., Mostofsky, S., Castellanos, F.X., Milham, M.P., 2012. Distinct neural signatures detected for ADHD subtypes after controlling for micro-movements in resting state functional connectivity MRI data. Front. Syst. Neurosci. 6, 80.

https://doi.org/10.3389/fnsys.2012.00080
Fonov, V., Evans, A.C., Botteron, K., Almli, C.R., McKinstry, R.C., Collins, D.L., Brain Development Cooperative Group, 2011. Unbiased average age-appropriate atlases for pediatric studies. Neuroimage 54, 313–327. https://doi.org/10.1016/j.neuroimage.2010.07.033
Fox, M.D., Corbetta, M., Snyder, A.Z., Vincent, J.L., Raichle, M.E., 2006. Spontaneous neuronal activity distinguishes human dorsal and ventral attention systems. Proc. Natl. Acad. Sci. U. S. A. 103, 10046–10051. https://doi.org/10.1073/pnas.0604187103
Fox, M.D., Zhang, D., Snyder, A.Z., Raichle, M.E., 2009. The global signal and observed anticorrelated resting state brain networks. J. Neurophysiol. 101, 3270–3283. https://doi.org/10.1152/jn.90777.2008
Friston, K.J., Williams, S., Howard, R., Frackowiak, R.S., Turner, R., 1996. Movement-related effects in fMRI time-series. Magn. Reson. Med. 35, 346–355. https://doi.org/10.1002/mrm.1910350312
Gajjar, A., Sanford, R.A., Heideman, R., Jenkins, J.J., Walter, A., Li, Y., Langston, J.W., Muhlbauer, M., Boyett, J.M., Kun, L.E., 1997. Low-grade astrocytoma: a decade of experience at St. Jude Children's Research Hospital. J. Clin. Oncol. 15, 2792–2799. https://doi.org/10.1200/JCO.1997.15.8.2792
Gratton, C., Koller, J.M., Shannon, W., Greene, D.J., Maiti, B., Snyder, A.Z., Petersen, S.E., Perlmutter, J.S., Campbell, M.C., 2019. Emergent Functional Network Effects in Parkinson Disease. Cereb. Cortex 29, 2509–2523. https://doi.org/10.1093/cercor/bhy121
Greene, D.J., Laumann, T.O., Dubis, J.W., Ihnen, S.K., Neta, M., Power, J.D., Pruett, J.R., Jr, Black, K.J., Schlaggar, B.L., 2014. Developmental changes in the organization of functional connections between the basal ganglia and cerebral cortex. J. Neurosci. 34, 5842–5854. https://doi.org/10.1523/JNEUROSCI.3069-13.2014
Gupta, P., Jalali, R., 2017. Long-term Survivors of Childhood Brain Tumors: Impact on General Health and Quality of Life. Curr. Neurol. Neurosci. Rep. 17, 99. https://doi.org/10.1007/s11910-017-0808-0
Hardy, K.K., Willard, V.W., Gioia, A., Sharkey, C., Walsh, K.S., 2018. Attention-mediated neurocognitive profiles in survivors of pediatric brain tumors: comparison to children with neurodevelopmental ADHD. Neuro. Oncol. 20, 705–715. https://doi.org/10.1093/neuonc/nox174
Hojjati, S.H., Ebrahimzadeh, A., Babajani-Feremi, A., 2019. Identification of the Early Stage of Alzheimer's Disease Using Structural MRI and Resting-State fMRI. Front. Neurol. 10, 904. https://doi.org/10.3389/fneur.2019.00904
Kazumata, K., Tha, K.K., Uchino, H., Ito, M., Nakayama, N., Abumiya, T., 2017. Mapping altered brain connectivity and its clinical associations in adult moyamoya disease: A resting-state functional MRI study. PLoS One 12, e0182759. https://doi.org/10.1371/journal.pone.0182759
King, A.A., Seidel, K., Di, C., Leisenring, W.M., Perkins, S.M., Krull, K.R., Sklar, C.A., Green, D.M., Armstrong, G.T., Zeltzer, L.K., Wells, E., Stovall, M., Ullrich, N.J., Oeffinger, K.C., Robison, L.L., Packer, R.J., 2017. Long-term neurologic health and psychosocial function of adult survivors of childhood medulloblastoma/PNET: a

report from the Childhood Cancer Survivor Study. Neuro. Oncol. 19, 689–698. https://doi.org/10.1093/neuonc/now242

Krull, K.R., Hardy, K.K., Kahalley, L.S., Schuitema, I., Kesler, S.R., 2018. Neurocognitive Outcomes and Interventions in Long-Term Survivors of Childhood Cancer. J. Clin. Oncol. 36, 2181–2189. https://doi.org/10.1200/JCO.2017.76.4696

La Rosa, P.S., Brooks, T.L., Deych, E., Shands, B., Prior, F., Larson-Prior, L.J., Shannon, W.D., 2016. Gibbs distribution for statistical analysis of graphical data with a sample application to fcMRI brain images. Stat. Med. 35, 566–580. https://doi.org/10.1002/sim.6757

Laumann, T.O., Gordon, E.M., Adeyemo, B., Snyder, A.Z., Joo, S.J., Chen, M.-Y., Gilmore, A.W., McDermott, K.B., Nelson, S.M., Dosenbach, N.U.F., Schlaggar, B.L., Mumford, J.A., Poldrack, R.A., Petersen, S.E., 2015. Functional System and Areal Organization of a Highly Sampled Individual Human Brain. Neuron 87, 657–670. https://doi.org/10.1016/j.neuron.2015.06.037

Leuthardt, E.C., Guzman, G., Bandt, S.K., Hacker, C., Vellimana, A.K., Limbrick, D., Milchenko, M., Lamontagne, P., Speidel, B., Roland, J., Miller-Thomas, M., Snyder, A.Z., Marcus, D., Shimony, J., Benzinger, T.L.S., 2018. Integration of resting state functional MRI into clinical practice - A large single institution experience. PLoS One 13, e0198349. https://doi.org/10.1371/journal.pone.0198349

Matthews, P.M., Honey, G.D., Bullmore, E.T., 2006. Applications of fMRI in translational medicine and clinical practice. Nat. Rev. Neurosci. 7, 732–744. https://doi.org/10.1038/nrn1929

Merchant, T.E., Li, C., Xiong, X., Kun, L.E., Boop, F.A., Sanford, R.A., 2009. Conformal radiotherapy after surgery for paediatric ependymoma: a prospective study. Lancet Oncol. 10, 258–266. https://doi.org/10.1016/S1470-2045(08)70342-5

Packer, R.J., Gajjar, A., Vezina, G., Rorke-Adams, L., Burger, P.C., Robertson, P.L., Bayer, L., LaFond, D., Donahue, B.R., Marymont, M.H., Muraszko, K., Langston, J., Sposto, R., 2006. Phase III study of craniospinal radiation therapy followed by adjuvant chemotherapy for newly diagnosed average-risk medulloblastoma. J. Clin. Oncol. 24, 4202–4208. https://doi.org/10.1200/JCO.2006.06.4980

Pizoli, C.E., Shah, M.N., Snyder, A.Z., Shimony, J.S., Limbrick, D.D., Raichle, M.E., Schlaggar, B.L., Smyth, M.D., 2011. Resting-state activity in development and maintenance of normal brain function. Proc. Natl. Acad. Sci. U. S. A. 108, 11638–11643. https://doi.org/10.1073/pnas.1109144108

Posner, M.I., Petersen, S.E., 1990. The attention system of the human brain. Annu. Rev. Neurosci. 13, 25–42. https://doi.org/10.1146/annurev.ne.13.030190.000325

Power, J.D., Cohen, A.L., Nelson, S.M., Wig, G.S., Barnes, K.A., Church, J.A., Vogel, A.C., Laumann, T.O., Miezin, F.M., Schlaggar, B.L., Petersen, S.E., 2011. Functional network organization of the human brain. Neuron 72, 665–678. https://doi.org/10.1016/j.neuron.2011.09.006

Power, J.D., Mitra, A., Laumann, T.O., Snyder, A.Z., Schlaggar, B.L., Petersen, S.E., 2014. Methods to detect, characterize, and remove motion artifact in resting state fMRI. Neuroimage 84, 320–341. https://doi.org/10.1016/j.neuroimage.2013.08.048

Ris, M.D., Leisenring, W.M., Goodman, P., Di, C., Noll, J., Levy, W., Robison, L.L., Armstrong, G.T., 2019. Neuropsychological and socioeconomic outcomes in adult survivors of pediatric low-grade glioma. Cancer 125, 3050–3058.

https://doi.org/10.1002/cncr.32186
Roland, J.L., Griffin, N., Hacker, C.D., Vellimana, A.K., Akbari, S.H., Shimony, J.S., Smyth, M.D., Leuthardt, E.C., Limbrick, D.D., 2017. Resting-state functional magnetic resonance imaging for surgical planning in pediatric patients: a preliminary experience. J. Neurosurg. Pediatr. 20, 583–590. https://doi.org/10.3171/2017.6.PEDS1711
Schulte, F., Kunin-Batson, A.S., Olson-Bullis, B.A., Banerjee, P., Hocking, M.C., Janzen, L., Kahalley, L.S., Wroot, H., Forbes, C., Krull, K.R., 2019. Social attainment in survivors of pediatric central nervous system tumors: a systematic review and meta-analysis from the Children's Oncology Group. J. Cancer Surviv. 13, 921–931. https://doi.org/10.1007/s11764-019-00808-3
Seitzman, B.A., Gratton, C., Marek, S., Raut, R.V., Dosenbach, N.U.F., Schlaggar, B.L., Petersen, S.E., Greene, D.J., 2020. A set of functionally-defined brain regions with improved representation of the subcortex and cerebellum. Neuroimage 116290. https://doi.org/10.1016/j.neuroimage.2019.116290
Seitzman, B.A., Snyder, A.Z., Leuthardt, E.C., Shimony, J.S., 2019. The State of Resting State Networks. Top. Magn. Reson. Imaging 28, 189–196. https://doi.org/10.1097/RMR.0000000000000214
Shah, M.N., Mitra, A., Goyal, M.S., Snyder, A.Z., Zhang, J., Shimony, J.S., Limbrick, D.D., Raichle, M.E., Smyth, M.D., 2018. Resting state signal latency predicts laterality in pediatric medically refractory temporal lobe epilepsy. Childs. Nerv. Syst. 34, 901–910. https://doi.org/10.1007/s00381-018-3770-5
Siegel, J.S., Mitra, A., Laumann, T.O., Seitzman, B.A., Raichle, M., Corbetta, M., Snyder, A.Z., 2017. Data Quality Influences Observed Links Between Functional Connectivity and Behavior. Cereb. Cortex 27, 4492–4502. https://doi.org/10.1093/cercor/bhw253
Siegel, J.S., Seitzman, B.A., Ramsey, L.E., Ortega, M., Gordon, E.M., Dosenbach, N.U.F., Petersen, S.E., Shulman, G.L., Corbetta, M., 2018. Re-emergence of modular brain networks in stroke recovery. Cortex 101, 44–59. https://doi.org/10.1016/j.cortex.2017.12.019
Smith, S.M., Jenkinson, M., Woolrich, M.W., Beckmann, C.F., Behrens, T.E.J., Johansen-Berg, H., Bannister, P.R., De Luca, M., Drobnjak, I., Flitney, D.E., Niazy, R.K., Saunders, J., Vickers, J., Zhang, Y., De Stefano, N., Brady, J.M., Matthews, P.M., 2004. Advances in functional and structural MR image analysis and implementation as FSL. Neuroimage 23 Suppl 1, S208–19. https://doi.org/10.1016/j.neuroimage.2004.07.051
van den Heuvel, M.P., Hulshoff Pol, H.E., 2010. Exploring the brain network: a review on resting-state fMRI functional connectivity. Eur. Neuropsychopharmacol. 20, 519–534. https://doi.org/10.1016/j.euroneuro.2010.03.008
Zeltzer, L.K., Recklitis, C., Buchbinder, D., Zebrack, B., Casillas, J., Tsao, J.C.I., Lu, Q., Krull, K., 2009. Psychological status in childhood cancer survivors: a report from the Childhood Cancer Survivor Study. J. Clin. Oncol. 27, 2396–2404. https://doi.org/10.1200/JCO.2008.21.1433